THE JOURNAL OF BIOLOGICAL CHEMISTRY VOL. 285, NO. 2, pp. 1272–1282, January 8, 2010


# Interaction of Double-stranded RNA-dependent Protein Kinase (PKR) with the Death Receptor Signaling Pathway in Amyloid β (Aβ)-treated Cells and in $APP_{SL}$PS1 Knock-in Mice*[S]

Received for publication, July 16, 2009, and in revised form, October 27, 2009 Published, JBC Papers in Press, November 4, 2009, DOI 10.1074/jbc.M109.041954

**Julien Couturier[‡], Milena Morel[‡], Raymond Pontcharraud[‡], Virginie Gontier[‡], Bernard Fauconneau[‡], Marc Paccalin[‡§¶], and Guylène Page[‡1]**

*From the [‡]Research Group on Brain Aging, GReViC EA 3808, University of Poitiers, 6 rue de la Milétrie, BP 199, 86034 Poitiers Cedex, France, the [§]Department of Geriatrics, Poitiers University Hospital, 2 rue de la Milétrie, BP 577, 86021 Poitiers Cedex, France, and the [¶]Clinical Investigation Center, CIC INSERM 802, Poitiers University Hospital, Poitiers, France*

**For 10 years, research has focused on signaling pathways controlling translation to explain neuronal death in Alzheimer Disease (AD). Previous studies demonstrated in different cellular and animal models and AD patients that translation is down-regulated by the activation of double-stranded RNA-dependent protein kinase (PKR). Among downstream factors of PKR, the Fas-associated protein with a death domain (FADD) and subsequent activated caspase-8 are responsible for PKR-induced apoptosis in recombinant virus-infected cells. However, no studies have reported the role of PKR in death receptor signaling in AD. The aim of this project is to determine physical and functional interactions of PKR with FADD in amyloid-β peptide (Aβ) neurotoxicity and in $APP_{SL}$PS1 KI transgenic mice. In SH-SY5Y cells, results showed that Aβ42 induced a large increase in phosphorylated PKR and FADD levels and a physical interaction between PKR and FADD in the nucleus, also observed in the cortex of $APP_{SL}$PS1 KI mice. However, PKR gene silencing or treatment with a specific PKR inhibitor significantly prevented the increase in $pT^{451}$-PKR and $pS^{194}$-FADD levels in SH-SY5Y nuclei and completely inhibited activities of caspase-3 and -8. The contribution of PKR in neurodegeneration through the death receptor signaling pathway may support the development of therapeutics targeting PKR to limit neuronal death in AD.**

Alzheimer Disease (AD)[2] is the leading cause of dementia in the elderly, affecting 25 million people in the world with about 5% of genetic origin. The biological features of AD are neuronal loss, senile plaques predominantly composed of amyloid β peptide (Aβ), and the presence of neurofibrillary tangles, leading to a progressive deterioration of cognitive function with loss of memory. Unfortunately, no definitive therapy for AD exists. The involvement of Aβ is clearly established, but mechanisms that underlie neuronal death are currently under investigation. For 10 years, research has focused on pathways controlling translation (1–5). They revealed that activated double-stranded RNA-dependent protein kinase (PKR), which phosphorylates the α-subunit of eIF2, was associated with degenerating neurons in AD brains (6–8). Furthermore, the levels of phosphorylated forms of PKR and eIF2α were significantly increased in AD cellular models exposed to Aβ42 (2, 5) in the brain of AD transgenic mice (1, 9) and in lymphocytes of AD patients (10). These modifications were negatively correlated with cognitive and memory test scores performed in AD patients (3, 10, 11). Besides its important role as a translational regulator, PKR is a key mediator in different signaling pathways. Indeed, among its downstream targets, the Fas-associated protein with a death domain (FADD) and subsequent caspase-8 are responsible for PKR-induced apoptosis in virus-infected cells (12). Furthermore, the overexpression of a dominant-negative FADD construct rescued SH-SY5Y cells from either tumor necrosis factor (TNF)-related apoptosis-inducing ligand (TRAIL) or Aβ-induced neurotoxicity (13). FADD could be involved in apoptosis through its nuclear localization by interacting with the methyl-CpG binding domain protein 4 (MDB4), a protein known to be implicated in DNA repair, but that could promote apoptosis when associated with FADD (14). Furthermore, many post-mortem studies have reported the role of the FADD-linked death receptor signaling pathway in the pathobiology of AD (15–17).

However, control of FADD under the PKR activation in AD remains unknown. The present study performed a detailed analysis of PKR and FADD interaction in Aβ-treated cells and in $APP_{SL}$PS1 KI transgenic mice. The purpose is to determine if inhibition of PKR could reduce apoptosis through the decrease in this death adaptor activation. Here, we showed a physical interaction between PKR and FADD in nuclei of Aβ42-treated SH-SY5Y and in $APP_{SL}$PS1 KI mice. Furthermore, PKR inhibitory treatments prevented not only the nuclear translocation of FADD but also significantly decreased caspase-3 and -8 activities induced by Aβ neurotoxicity.

## EXPERIMENTAL PROCEDURES

*Materials*—All-*trans* retinoic acid (RA), sterile-filtered dimethyl sulfoxide Hybri-Max® (DMSO), paraformaldehyde

* This work was supported by grants from the Association Internationale pour la Recherche sur la Maladie d'Alzheimer (AIRMA) and Association France Alzheimer.

[S] The on-line version of this article (available at http://www.jbc.org) contains supplemental Figs. S1 and S2.

[1] To whom correspondence should be addressed. Tel.: 33-5-49-36-62-60; Fax: 33-5-49-36-62-63; E-mail: guylene.page@univ-poitiers.fr.

[2] The abbreviations used are: AD, Alzheimer disease; PKR, double-stranded RNA-dependent protein kinase; Aβ, amyloid β; PMSF, phenylmethylsulfonyl fluoride; DAPI, 4′,6-diamidino-2-phenylindole; PBS, phosphate-buffered saline; TRITC, tetramethylrhodamine isothiocyanate; FITC, fluorescein isothiocyanate; FADD, Fas-associated protein with a death domain; ANOVA, analysis of variance; KI, knock-in; RA, retinoic acid; IP, immunoprecipitation.

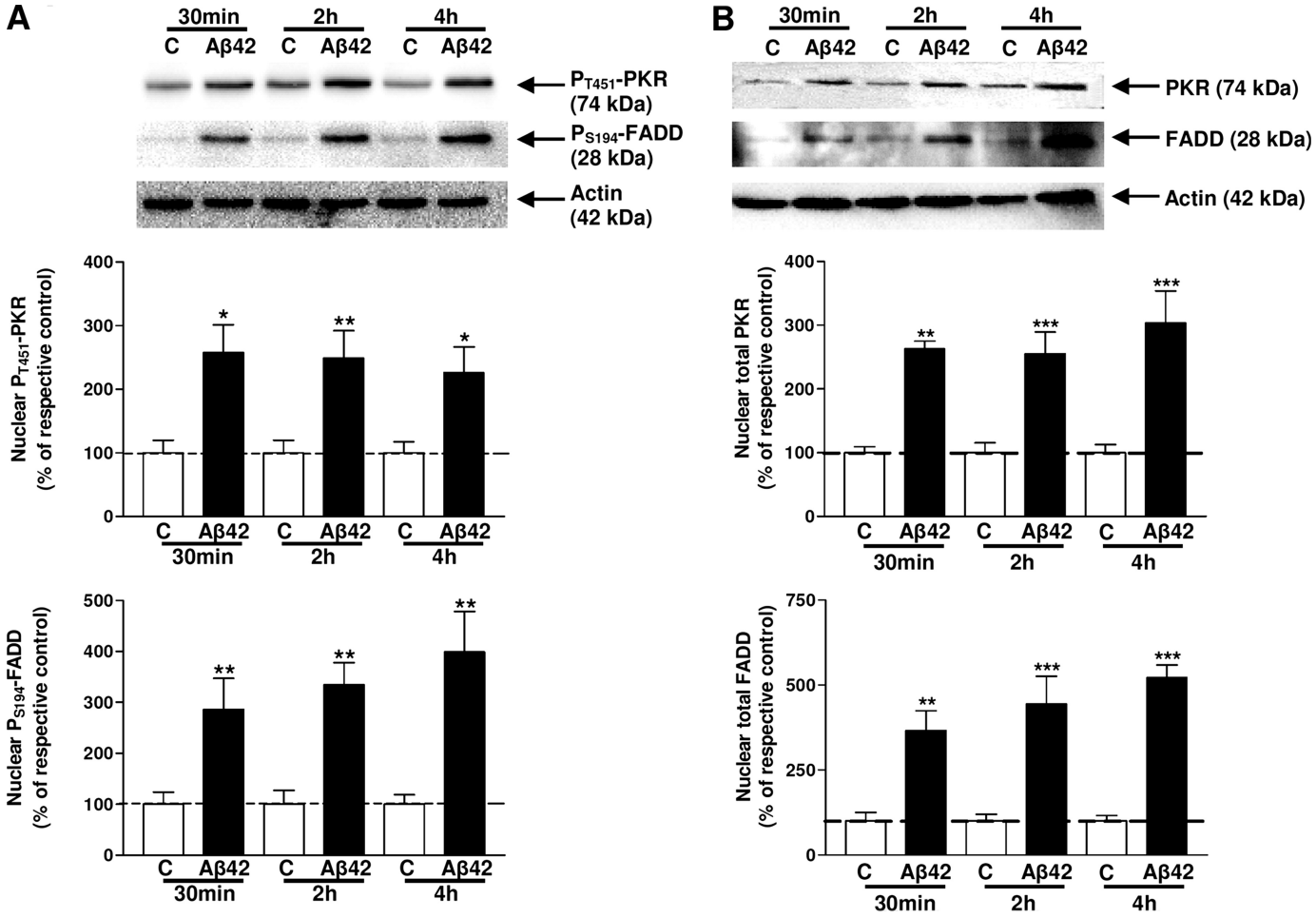


FIGURE 1. **Immunoreactivities of PKR and FADD in nuclear extracts of SH-SY5Y cells.** Representative blots showed the immunoreactivity of $pT^{451}$-PKR and $pS^{194}$-FADD (*A*), total PKR and total FADD (*B*) and corresponding actin in nuclear extracts of Aβ42-treated SH-SY5Y cells. Data are reported to those of the corresponding actin. The results are expressed as arbitrary units and are normalized compared with the respective time control. Results are mean ± S.E. from five independent experiments in duplicate. *, $p < 0.05$; **, $p < 0.01$; and ***, $p < 0.001$ compared with the respective control by one-way ANOVA followed by Newman-Keuls' test for multiple comparisons.

(PFA), glutaraldehyde, sodium citrate, Triton X-100, bovine serum albumin, sodium fluoride (NaF), phenylmethylsulfonyl fluoride (PMSF), protease and phosphatase inhibitors, dithiothreitol, 4′,6-diamidino-2-phenylindole dihydrochloride (DAPI), and acrylamide were obtained from Sigma. Human β-amyloid peptide [Aβ 1–42], positive C16 compound [(+)C16], and negative C16 compound [(−)C16] were purchased from Merck Chemicals, all reagent-grade chemicals for buffers from VWR International (Strasbourg, France), and those for cell culture from Invitrogen (Cergy Pontoise, France). All primary antibodies and the secondary anti-rabbit IgG antibody conjugated with horseradish peroxidase were purchased from Cell Signaling (Ozyme distributor, St. Quentin Yvelines, France) except for anti-Fas L and anti-amyloid peptide (clone 4G8) from Chemicon (Millipore distributor, St-Quentin-en-Yvelines, France), anti-β-tubulin and anti-actin from Sigma, peroxidase-conjugated anti-mouse IgG from Amersham Biosciences, GE Healthcare (Orsay, France). For immunocytochemistry, anti-$pS^{194}$-FADD was obtained from Santa Cruz Biotechnology (Tebu-Bio Distributor, Le Perray en Yvelines, France). For immunoprecipitation, the antibodies against total PKR and those anti-total FADD came from Cell Signaling and from Affinity BioReagents (Ozyme Distributor).

*SH-SY5Y Culture*—The SH-SY5Y neuroblastoma cell line obtained from ATTC were propagated in minimum essential medium (MEM) mixed with F12 (1:1, v/v), and supplemented with 10% heat-inactivated fetal bovine serum (FBS) and 1% penicillin-streptomycin (PS). The cells were cultured in 6-well plates and maintained in a humidified 5% $CO_2$ atmosphere at 37 °C. Cells (600,000 cells per well) were differentiated into neural cells by incubating with 10 μM RA for 7 days as previously described (2).

*In Vitro siRNA Transfection Protocol*—PKR siRNA and Lit28i siRNA as a negative control were generated by Biolabs (Ozyme distributor, St. Quentin Yvelines, France). The best percentage of transfected cells obtained was 78 ± 4% ($n = 4$ in duplicate) using 5 nM fluorescein-siRNA, 8 μl of the Interferin™ transfection reagent, and 48 h of incubation. The Interferin™-siRNA mix was directly added to cells seeded at 60% confluency in 2 ml of fresh medium, and 6-well plates were incubated at 37 °C for 48 h before Aβ42 treatment. These experimental conditions showed a decrease in PKR protein levels of 34.01 ± 5.13% ($n = 6$ independent experiments).

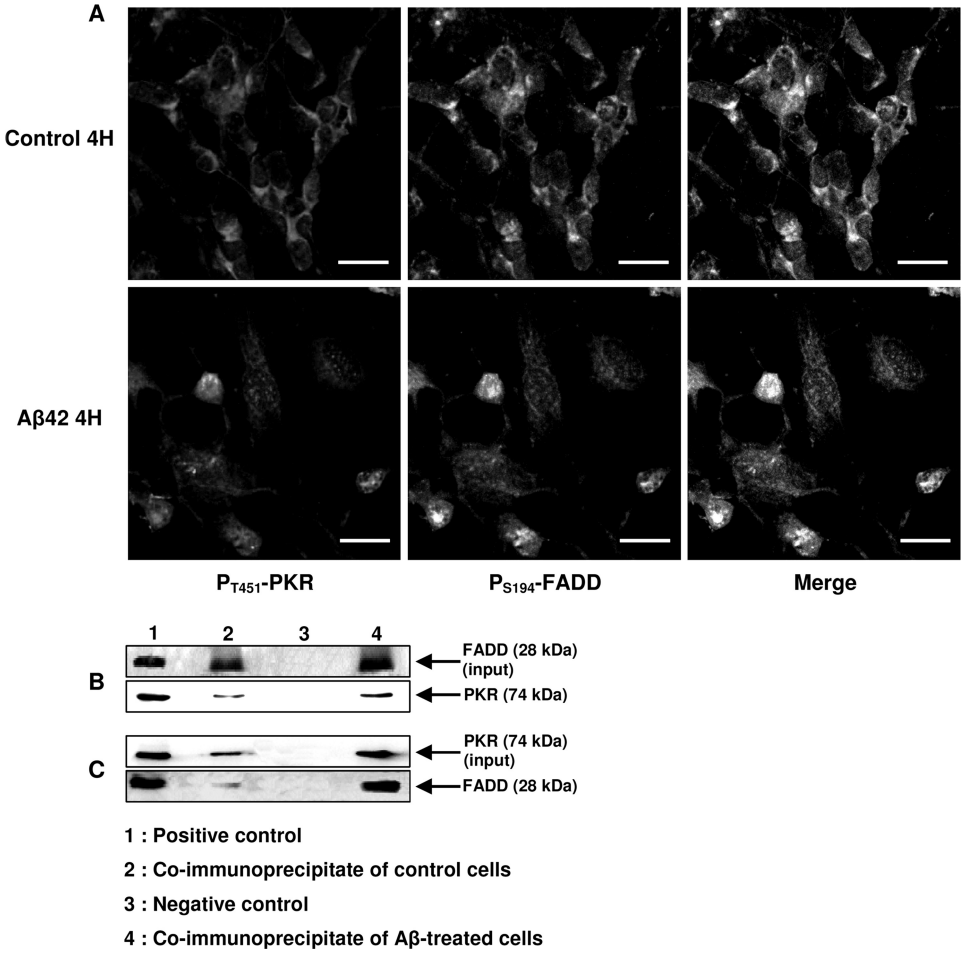


FIGURE 2. **Physical interaction between PKR and FADD in SH-SY5Y cells.** Confocal staining of $pT^{451}$-PKR and $pS^{194}$-FADD in Aβ42-treated SH-SY5Y for 4 h (*A*). A clear nuclear co-localization of $pT^{451}$-PKR and $pS^{194}$-FADD was depicted in Aβ42-treated cells. Photographs are representative of five experiments in duplicate. *Bars*: 20 μm. *B* and *C*, co-IP of FADD and PKR using the ExactaCruz™ kit. Nuclear extracts from Aβ42-treated SH-SY5Y (*lane 4*) were subjected to IP with the anti-FADD antibody-IP matrix complex, and the blot shows the band of PKR as in the positive control corresponding to nuclear extracts not immunoprecipitated (*lane 1*, *B*). Nuclear extracts of Aβ42-treated cells were incubated with the anti-total PKR antibody-IP matrix complex, and the blot shows the band of FADD as in the positive control (*C*). Co-IP of control cells show weak signals (*lane 2*, *B* and *C*). In *lane 3*, a negative control corresponded to nuclear extracts of Aβ42-treated SH-SY5Y cells immunoprecipitated with mouse (*B*) or rabbit (*C*) ChromPure IgG antibody. For each co-IP, we included a blot of FADD (*B*) and PKR (*C*) input to evaluate the efficiency of the pull-down assay and the proportion of proteins that are bound to the IP matrix.

*Chemical Treatments*—Cells were exposed to 20 μM Aβ42 in serum-free medium and incubated for 30 min to 8 h. At this concentration, previous reports showed a significant activation of PKR in RA-differentiated SH-SY5Y cells (2, 5). In the same time, control cells were exposed to serum-free medium. The Aβ42 was diluted in sterile ultra-high-quality water ($H_2O_{UHQ}$). Then, prior to the treatment of SH-SY5Y cells, Aβ42 was incubated 48 h at 37 °C for aggregation as recommended by the Merck Chemical supplier (18). After treatment, medium was conserved to analyze Aβ42 monomers and oligomers by immunoblot and fibrillar form of Aβ42 by scanning electron microscopy under our experimental conditions (see supplemental Fig. S1). Results showed the presence of a mixture composed of monomers, oligomers (8, 12, and 16 kDa), and fibrils. Because the specific toxicity of these different states of Aβ was not clearly demonstrated, we decided to incubate SH-SY5Y cells with the whole mixture.

The (+)C16 compound was a specific PKR inhibitor (19). Cells were exposed to 2 μM C16 dissolved in 2% DMSO and added in serum-free medium for 1 h before Aβ42 treatment. Then, a set of SH-SY5Y cells was exposed to 2 μM of negative PKR inhibitor [(−)C16] and another set to 2% DMSO (vehicle of the C16 compound) under the same experimental conditions.

*Preparation of Cell Lysates and Both Nuclear and Cytoplasmic Extracts*—After treatments, cells were washed with phosphate-buffered saline (PBS: 154 mM NaCl, 1.54 mM $KH_2PO_4$, 2.7 mM $Na_2HPO_4 \cdot 7H_2O$, pH 7.2) and lysed in ice-cold lysis buffer (50 mM Tris-HCl, 50 mM NaCl pH 6.8, 1% (v/v) Triton X-100, 1 mM PMSF, 50 mM NaF, 1% (v/v) protease inhibitor mixture, and 1% (v/v) phosphatase inhibitor mixture). Lysates were centrifuged at 15,000 × *g* for 15 min at 4 °C.

For nuclear extracts, the procedure was based on the protocol described previously (20) with some modifications. Cells were centrifuged at 5,500 × *g* for 10 min at 4 °C. The pellet was lysed in cytoplasmic lysis buffer (10 mM Hepes, pH 7.9, 10 mM KCl, 0.1 mM EDTA, 0.1 mM EGTA, 1 mM dithiothreitol, 0.5 mM PMSF, and 10% Igepal) and was centrifuged at 11,000 × *g* for 10 min at 4 °C. The cytoplasmic fraction was isolated, and the nuclear pellet was lysed in nuclear lysis buffer (20 mM Hepes pH 7.9, 400 mM NaCl, 1 mM EDTA, 1 mM EGTA, 1 mM dithiothreitol, and 0.5 mM PMSF) for 2 h at 4 °C. Then, vials were centrifuged at 1,600 × *g* for 5 min at 4 °C, and the supernatant was isolated. In each lysis buffer, 1% of protease and 1% phosphatase inhibitor cocktails were extemporaneously added. The quantity of total protein was measured with the Bio-Rad protein assay kit.

*Transgenic Mice*—The generation of $APP_{SL}$PS1 KI mice has been described previously (21). In brief, these transgenic mice were generated by breeding homozygous PS1 KI mice (carrying M233T and L235P mutations known in familial early-onset forms of AD at 29 and 35 years of age, respectively) with hemizygous $APP_{SL}$ mice expressing human mutant $APP_{SL}$ (APP751 carrying the Swedish K670N/M671L and London V717I mutations, Thy1 promoter). A robust gender effect with female mice displaying more severe pathology with earlier neuronal loss at 6 months of age than male littermates has been observed (21). In total, female $APP_{SL}$PS1 KI mice at 3 months ($n = 6$) as well as

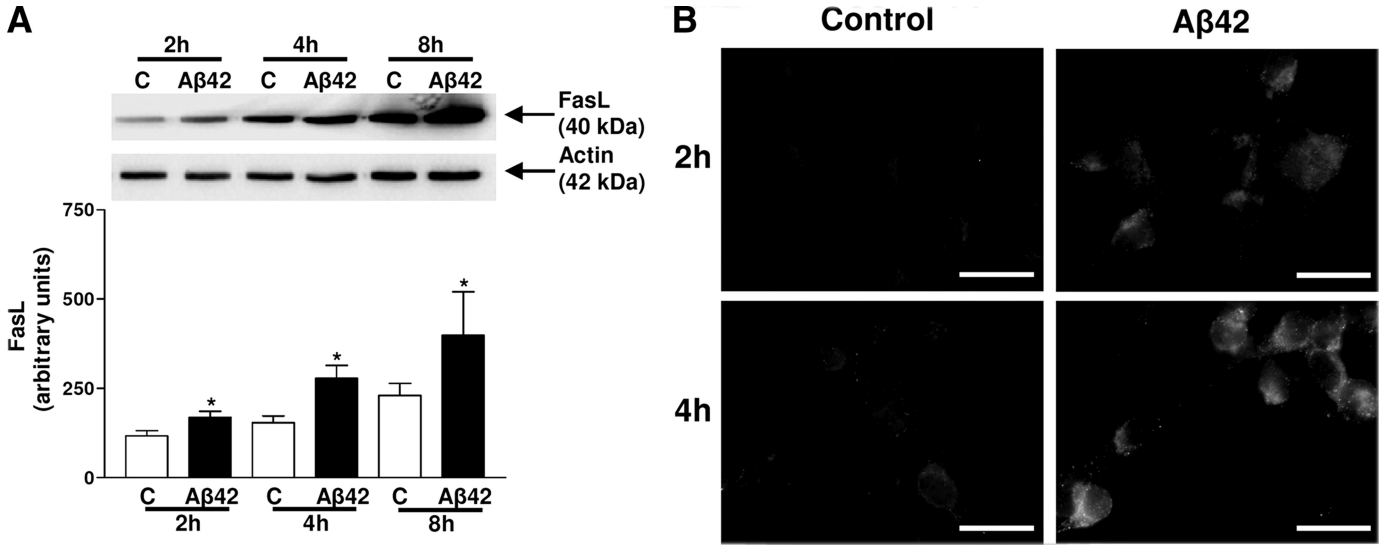


FIGURE 3. **Immunoreactivity of FasL in SH-SY5Y cells.** Representative blots show the immunoreactivity of FasL and actin in lysates of A$\beta$42-treated SH-SY5Y. Results are mean ± S.E. from five independent experiments. *, $p < 0.05$ compared with the respective control and †, $p < 0.05$ for control 2 h *versus* control 8 h, by one-way ANOVA followed by Newman-Keuls' test for multiple comparisons (*A*). Immunofluorescent staining of FasL in A$\beta$42-treated SH-SY5Y increased with the time incubation compared with the weak signal in the control. Photographs are representative of five experiments in duplicate. *Bars*: 20 $\mu$m (*B*).

age-matched wild-type controls ($n = 6$) were used (generous gift from Sanofi-Aventis, Vitry sur Seine, France). All animal experiments were performed in compliance and following approval of the Sanofi-Aventis Animal Care and Use Committee in accordance with standards of the guide for the care and use of laboratory animals (CNRS ILAR) and with respect to French and European Community rules. Brain tissue preparation was performed as previously described (9).

*Immunoblot*—Protein samples (20 $\mu$g per lane) were applied on 12% Tris-glycine polyacrylamide gels, and proteins were transferred to polyvinylidene difluoride membranes (Fisher). Blots were blocked for 2 h in Tris-buffered saline Tween-20 (TBST, 20 mM Tris-HCl, 150 mM NaCl, pH 7.5, 0.05% Tween 20) containing 5% nonfat milk and 0.21% NaF. Membranes were incubated with primary antibody in blocking buffer at 4 °C overnight. The primary antibodies used were rabbit anti-pS$^{194}$-FADD for human and anti-pS$^{191}$-FADD for mouse (1:500), rabbit anti-FADD (1:500), rabbit anti-pT$^{451}$-PKR (1:500), rabbit anti-PKR (1:1000), rabbit anti-FasL (1:250), mouse anti-actin or anti-$\beta$-tubulin (1:100000 and 1:10000, respectively). After washes, membranes were incubated with horseradish peroxidase secondary antibody either anti-rabbit (1:1000) or anti-mouse (1:1000) for 1 h at room temperature. After washes, membranes were exposed to ECL plus (Amersham Biosciences). Chemiluminescence was captured by the G:Box real-time imaging system (Syngene). Automatic image analysis software is supplied with Gene Tools (Syngene). Data for each protein were compared to data of the corresponding actin or $\beta$-tubulin. Then, the ratio of phosphorylated protein/total protein was calculated to determine the level of the protein activation in mouse brain homogenates.

*Immunoprecipitation (IP)*—IP from SH-SY5Y nuclear extracts (100 $\mu$g of protein) or mouse cortex homogenates (200 $\mu$g of protein) was performed using 2.5 $\mu$g of IP antibody (anti-PKR or anti-FADD) according to the manufacturer's protocol with ExactaCruz$^{TM}$ kit (TebuBio). The positive control corresponded to nuclear extracts of A$\beta$42-treated SH-SY5Y cells or $APP_{SL}$PS1 KI cortex homogenates not immunoprecipitated and the negative control to nuclear extracts of A$\beta$42-treated SH-SY5Y cells or $APP_{SL}$PS1 KI cortex homogenates immunoprecipitated with rabbit (negative control for PKR) or mouse (negative control for FADD) ChromPure IgG antibody (Jackson ImmunoResearch).

*Caspase Activities*—Activities of caspase-3 and -8 were performed using two independent Caspase-Glo® assays purchased from Promega. A SH-SY5Y cell number of 5,000 and 10,000 cells/well was cultured in a 96-well plate for caspase-3 and -8, respectively. The protocol followed was similar for both kits according to the supplier. The cleavage of the luminogenic substrate containing the DEVD sequence or the LETD sequence selective for caspase-3 and -8, respectively, generated a "glow-type" luminescent signal recorded at 3 h for caspase-3 and 1 h for caspase-8 using the Packard lumiCount microplate luminometer (PerkinElmer).

*Immunofluorescence*—For FasL staining, cells were fixed with 4% PFA for 10 min and permeabilized with TBS (Tris 50 mM, NaCl 150 mM, pH 7.6)/0.3% Triton X-100 for 5 min at room temperature. Nonspecific sites were blocked with TBS, 5% BSA for 1 h at room temperature. Coverslips were incubated with rabbit anti-FasL antibody (1:50) in TBS, 1% BSA overnight at 4 °C. Then, cells were incubated with secondary biotinylated anti-rabbit antibody and with streptavidin-FITC (1:50) for 1 h at room temperature (Dakocytomation). Microscopic visualization was performed using an Olympus DP70 digital camera and Olympus DP-soft (Olympus S.A., Rungis, France).

For confocal staining of pT$^{451}$-PKR and pS$^{194}$-FADD, cells were fixed with 100% methanol 15 min at −20 °C. After unmasking antigens with 10 mM citric acid (pH 6) at 70 °C, cells were permeabilized and blocked in PBS (137 mM NaCl, 2.7 mM KCl, 10 mM $Na_2HPO_4$, 1.7 mM $KH_2PO_4$, pH 7.4) containing 0.3% Triton X-100 and 5% donkey serum albumin (DSA) (Jackson Immunoresearch). Cells were incubated in antibodies rab-

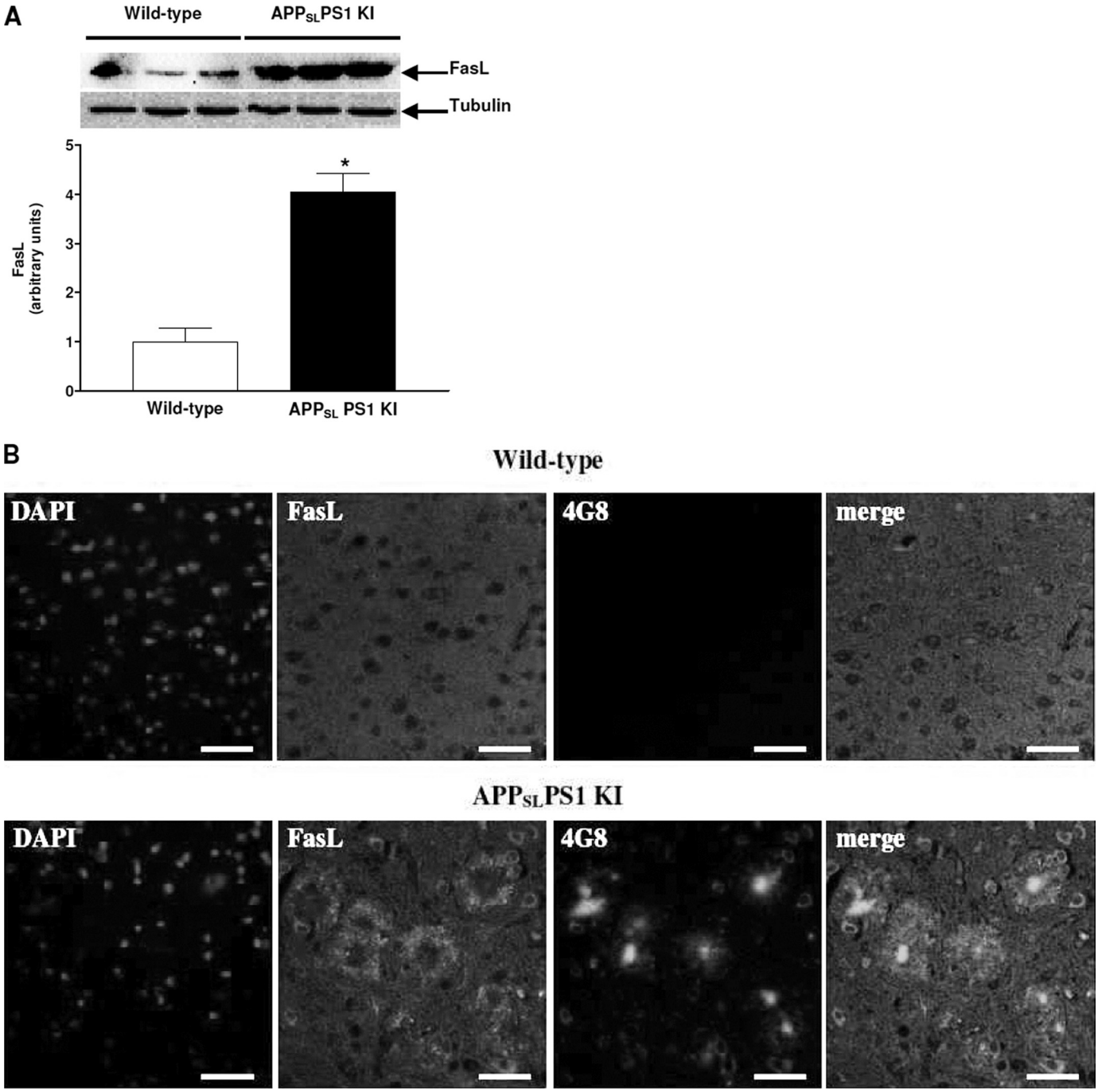


FIGURE 4. **Immunoreactivity of FasL in APP$_{SL}$PS1 KI mice.** *Panel A* shows the FasL levels in 3-month-old APP$_{SL}$PS1 KI mice compared with age-matched wild-type mice. Results are the mean ± S.E. of three mice in each group and expressed as arbitrary units. *, $p < 0.05$ compared with the wild-type group by a Mann Whitney test. *B*, in sagittal brain sections of APP$_{SL}$PS1 KI and wild-type mice, a triple confocal staining show that FasL was found not only around amyloid deposits as punctate spherical clusters but also co-localized with intracellular A$\beta$ in cortex compared with wild-type mouse without signal. The nuclei were dyed blue by DAPI. These photographs are representative of three mice in both groups. *Bars*: 40 $\mu$m.

bit anti- pT$^{451}$-PKR and goat anti-pS$^{194}$-FADD (both at dilution 1:50) in PBS/1% DSA/0,3% Triton X-100 overnight at 4 °C. Then, cells were incubated with anti-rabbit-TRITC and biotinylated anti-goat (1:50) for 1 h at room temperature. FITC-streptavidin (1:50) was added for 1 h at room temperature.

The immunofluorescence protocol for mouse brain sections was performed as previously described (22). 4-$\mu$m sagittal sections were first incubated 2 h at room temperature with the monoclonal mouse primary antibody to $\beta$-amyloid (4G8) at 1:100. After two washes in PBS, the A$\beta$ signal was detected using secondary Alexa-647-conjugated anti-mouse antibody at a final dilution 1:50 (Invitrogen). After two washes in PBS, a DAPI staining (1 $\mu$g/ml, 15 min) was performed before incubation of sections in the rabbit anti-FasL antibody (1:50) overnight at 4 °C. The amplification of FasL signal has been performed as described above for SH-SY5Y cells.

The labeled samples were examined with a spectral confocal FV-1000 station installed on an inverted microscope IX-81

(Olympus, Tokyo, Japan) with an Olympus UplanSapo ×60 water, 1.2 NA, objective lens. Fluorescence signal collection, image construction, and scaling were performed through the control software (Fluoview FV-AS10, Olympus). Multiple fluorescence signals were acquired sequentially to avoid cross-talk between image channels. Fluorophores were excited with 405 nm line of a diode (for DAPI), 488 nm line of an argon laser (for FITC), 543 nm line of an HeNe laser (for TRITC), and the 633 nm line of an HeNe laser (for Alexa-647). The emitted fluorescence were detected through spectral detection channels between 425 and 475 nm, 500 and 530 nm, and 555 and 625 nm, for blue, green, and red fluorescence respectively and through a 650-nm long pass filter for far red fluorescence. Images were then merged as an RGB image.

*Statistical Analysis*—Results are expressed as mean ± S.E. Data for multiple variable comparisons were analyzed by a one-way ANOVA followed by a Newman-Keuls' test as a post hoc test according to the statistical program GraphPad Instat (GraphPad Software, San Diego, CA). For two groups, a Mann Whitney test was performed. The level of significance was $p < 0.05$.

## RESULTS

*Physical Interaction between PKR and FADD in Aβ42-treated SH-SY5Y Cells*—Previous studies demonstrated that the $Thr^{451}$ phosphorylated site in the PKR activation loop was required *in vivo* and *in vitro* for high-level kinase activity (23). It has also been reported that the phosphorylation of the $Ser^{194}$ site of FADD protein is involved in activation (24) and the nuclear localization of FADD (25). $pT^{451}$-PKR and $pS^{194}$-FADD were analyzed in nuclear extracts of cells treated with 20 μM Aβ42 by immunoblot. The levels of $pT^{451}$-PKR were significantly increased at 30 min, 2 h, and 4 h (157, 149, and 126%, respectively) (Fig. 1*A*). Increases in $pS^{194}$-FADD levels were also detected after 30 min, 2 h, and 4 h of Aβ42 treatment (186, 234, and 299%, respectively) (Fig. 1*A*). At the same time, the cytoplasmic levels of $pT^{451}$-PKR (76, 71, and 82%, respectively) and $pS^{194}$-FADD (55, 72, and 72%, respectively) significantly decreased as those of their total forms (see supplemental Fig. S2), supporting the redistribution of $pT^{451}$-PKR and $pS^{194}$-FADD by Aβ42 treatment. In these two cellular compartments, total PKR and total FADD have the same profile as their phosphorylated form due to the translocation of $pT^{451}$-PKR and $pS^{194}$-FADD into the nucleus under this amyloid stress (Fig. 1*B*).

A confocal staining showed an intense expression of $pT^{451}$-PKR (red channel) and $pS^{194}$-FADD (green channel) in the nuclei of Aβ42-treated SH-SY5Y cells (Fig. 2*A*). In contrast, staining of $pT^{451}$-PKR and $pS^{194}$-FADD was weak and mainly co-localized in the cytoplasm of control cells. The ability of PKR to interact physically with FADD was tested by co-immunoprecipitation (IP) assays. After 4 h of exposure of SH-SY5Y cells to 20-μM Aβ42, nuclear extracts were subjected to IP with the anti-FADD antibody and immunoblot revealed a band of PKR as in the positive control non-immunoprecipitated (Fig. 2*B*). Conversely, IP with the anti-PKR antibody showed the presence of FADD (Fig. 2*C*). Co-IP assays of control nuclear extracts

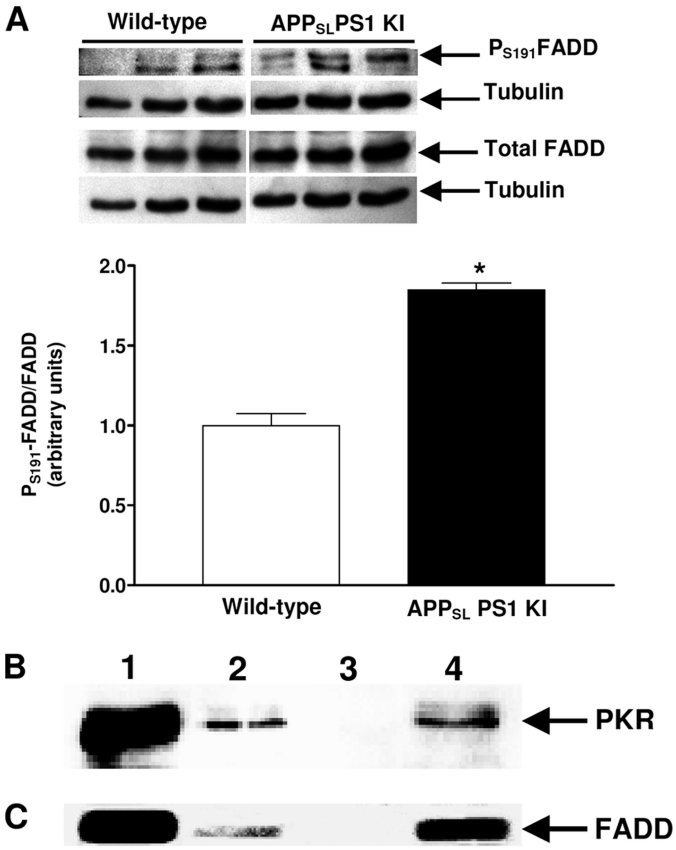


FIGURE 5. **Immunoreactivity of FADD and physical interaction with PKR in cortex of APP$_{SL}$PS1 KI mice.** In *A*, blots of $pS^{191}$-FADD and FADD are shown, and the ratios of $pS^{191}$-FADD/FADD are represented in the histogram. Results are the mean ± S.E. of three mice in each group and expressed as arbitrary units. *, $p < 0.05$ compared with the wild-type group by a Mann Whitney test. The blot *B* shows the signal of PKR after co-IP of FADD and blot *C* the signal of FADD after co-IP of PKR. Similar to Fig. 2, *lane 1* corresponds to the positive control, *lane 2* to the cortex of wild-type mice co-immunoprecipitated, *lane 3* to the negative control with mouse (*B*) or rabbit (*C*) ChromPure IgG antibody, and *lane 4* to the cortex of APP$_{SL}$PS1 KI mice co-immunoprecipitated.

revealed very weak signals (Fig. 2, *lane 2* in *B* and *C*). No band was observed in the negative control (Fig. 2, *lane 3* in *B* and *C*).

*FasL Expression in SH-SY5Y Cells Treated with Aβ42*—FasL expression was analyzed in lysates of SH-SY5Y cells after Aβ42 treatment for 2, 4, and 8 h by immunoblot. A significant increase in FasL amount was visualized after Aβ42 treatment (45, 80, and 73%, respectively) compared with control cells (Fig. 3*A*). A time-dependent increase of FasL expression was observed in control conditions probably because of incubation in serum-free medium, but this increase was statistically significant only for 2 h *versus* 8 h. Immunostaining depicted an intense FasL cytoplasmic signal in Aβ42-treated cells for 2 and 4 h (Fig. 3*B*) compared with respective controls incubated in serum-free medium.

*FasL Levels and Physical Interaction between PKR and FADD in APP$_{SL}$PS1 KI Mice*—These mice displayed a massive neuronal loss as early as 6 months of age with an intense neuronal apoptosis (9, 21). This neuronal loss distribution closely parallels the strong intraneuronal Aβ immunostaining and intracellular thioflavin-S-positive material but does not correlate with extracellular deposits (26). Therefore, we worked only with 3-month-old mice to examine abnormalities of death receptor

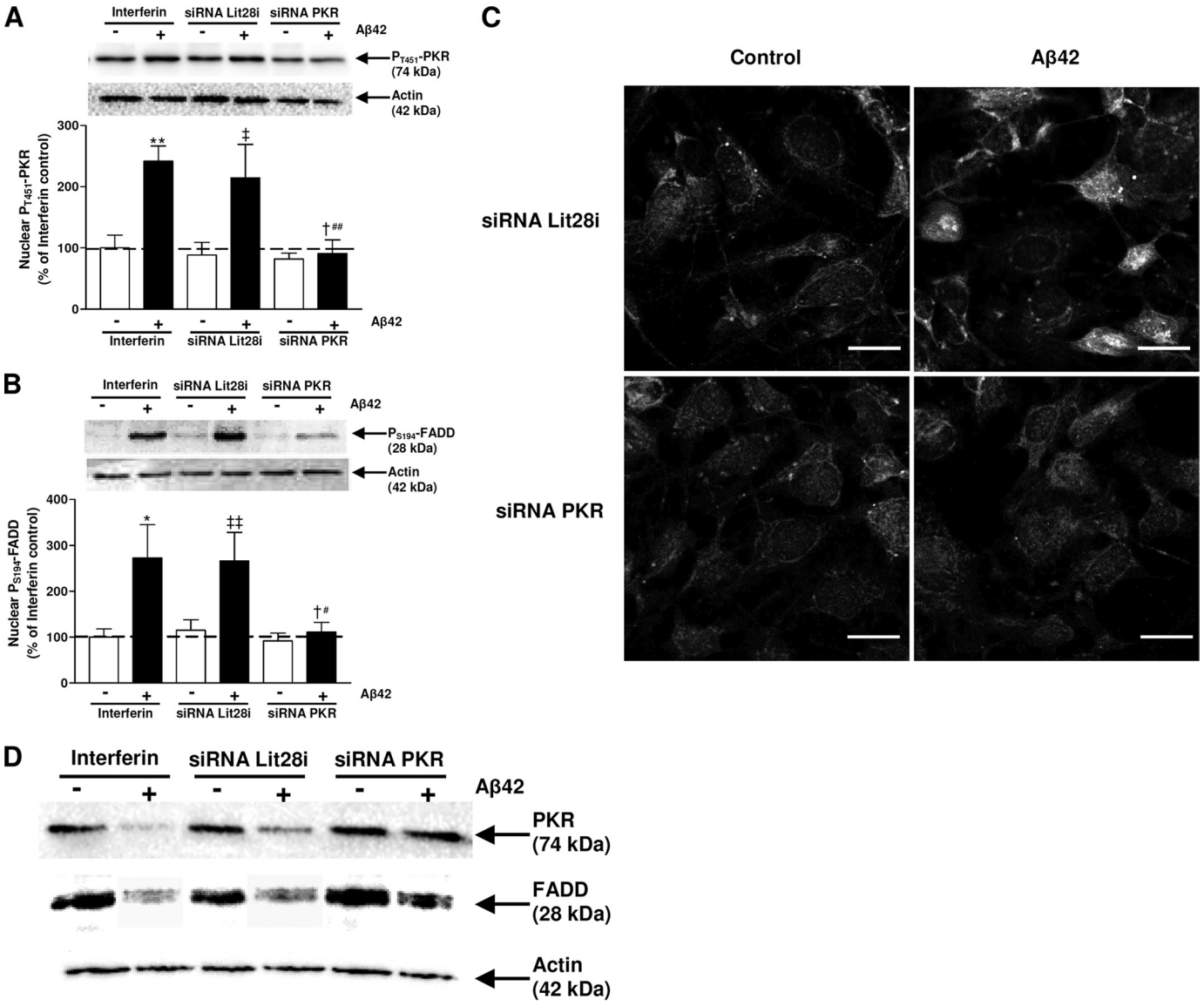


FIGURE 6. **Effects of PKR siRNA in A$\beta$42-treated cells.** Representative blots show the immunoreactivity of $pT^{451}$-PKR (*A*), $pS^{194}$-FADD (*B*) and actin in nuclear extracts from SH-SY5Y cells transfected either with Interferin™ or 5 nM Lit28i siRNA or 5 nM PKR siRNA for 48 h and then exposed to A$\beta$42 for 2 h. Results are expressed as arbitrary units and are normalized compared with Interferin™ control. Results are mean ± S.E. of five independent experiments. *, $p < 0.05$; **, $p < 0.01$ compared with Interferin™ control without A$\beta$42 treatment, ‡, $p < 0.05$; ‡‡, $p < 0.01$ compared with Lit28i siRNA without A$\beta$42 treatment; †, $p < 0.05$ compared with Lit28i siRNA + A$\beta$42 treatment; and #, $p < 0.05$; ##, $p < 0.01$ compared with Interferin™ + A$\beta$42 treatment by one-way ANOVA followed by Newman-Keuls' test for multiple comparisons. In *panel C*, a representative confocal staining of $pT^{451}$-PKR and $pS^{194}$-FADD in A$\beta$42-treated SH-SY5Y for 2 h show a robust signal in the nuclei, whereas transfection of PKR siRNA prevented $pT^{451}$-PKR and $pS^{194}$-FADD signals in the nuclei. *Bars*: 20 $\mu$m. In *panel D*, representative blots are shown of total PKR and total FADD and corresponding actin in cytoplasmic extracts from SH-SY5Y cells transfected either with Interferin™ or 5-nM Lit28i siRNA or 5 nM PKR siRNA for 48 h and then exposed to A$\beta$42 for 2 h.

signaling before neuronal loss. Experiments were performed with the cortex, where we showed a strong intraneuronal A$\beta$ accumulation and diffuse amyloid deposits at this age (27) and because the cortex offers sufficient material for all assays. In Fig. 4*A*, a large increase in FasL levels (305%) was observed in the cortex of $APP_{SL}$PS1 KI compared with wild-type mice. Immunostaining revealed FasL-positive clusters of spherical-appearing structures around amyloid deposits and intracellular co-localization of FasL and A$\beta$ in the cortex compared with the wild-type cortex (Fig. 4*B*). Furthermore, the ratio $pS^{191}$-FADD/FADD was significantly increased (85%) as was that of $pT^{451}$-PKR (previously published, Ref. 27) (Fig. 5*A*). Moreover, co-IP assays showed that PKR and FADD physically interacted in the cortex of $APP_{SL}$PS1 KI mice (Fig. 5, *B* and *C*) compared with co-immunoprecipitated wild-type cortex where signals were weak for PKR (Fig. 5, *line 2*, *panel B*) and absent for FADD (Fig. 5, *line 2*, *panel C*).

*Effect of PKR Gene Silencing Treatment in A$\beta$42-treated SH-SY5Y Cells*—Under our experimental conditions, a significant inhibition of $pT^{451}$-PKR levels (about 60%) was observed in nuclear extracts of PKR siRNA-transfected cells compared with those of cells transfected with Lit28i siRNA and to interferin™-transfected cells (Fig. 6*A*). Furthermore, the PKR gene silencing also led to a significant and similar reduction in $pS^{194}$-FADD compared with cells transfected with interferin™ or negative Lit28i siRNA and treated with A$\beta$42 for 2 h (Fig.

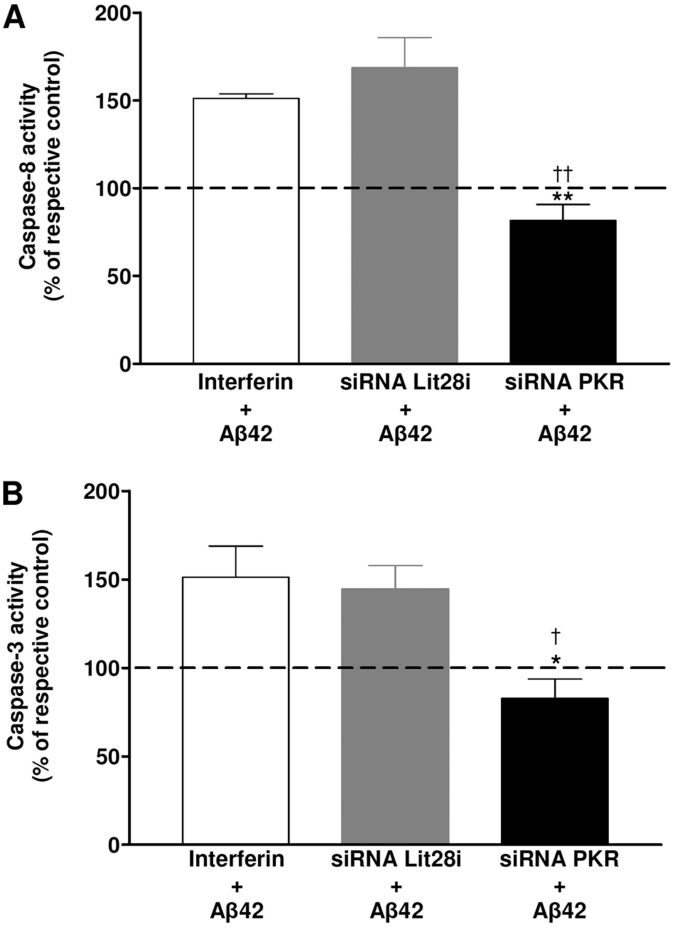


FIGURE 7. **Prevention of caspase-8 and -3 activities by PKR siRNA in Aβ42-treated SH-SY5Y cells.** Histograms show activities of caspase-8 (*A*) and -3 (*B*) after transfection of SH-SY5Y cells with either Interferin™ or Lit28i siRNA or PKR siRNA and Aβ42 treatment for 2 h. The addition of the specific luminogenic substrate of caspase-3 and -8 generated a luminescent signal reading by the luminometer. Under each condition and each experiment, the activity of caspase-8 and -3 obtained in the presence of Aβ was compared with that obtained without Aβ. Results represent the mean ± S.E. of five independent experiments in triplicate. Statistical analysis using a one-way ANOVA followed by the Newman-Keuls' test revealed significant results. *, $p < 0.05$; **, $p < 0.01$; and †, $p < 0.05$; ††, $p < 0.01$ compared with Interferin™- and Lit28i siRNA-transfected SH-SY5Y cells, respectively.

6*B*). Total forms of PKR and FADD in cytoplasmic extracts from SH-SY5Y cells transfected with 5 nM PKR siRNA for 48 h and exposed to Aβ42 for 2 h were comparable to those of cells not treated with Aβ42. When SH-SY5Y cells were transfected either with Interferin™ or 5-nM Lit28i siRNA and treated with Aβ42, the total forms of PKR and FADD decreased compared with corresponding cells not treated with Aβ42 (Fig. 6*D*).

A confocal staining showed that PKR gene silencing induced a consistent reduction in both $pT^{451}$-PKR and $pS^{194}$-FADD signals in the nuclei of Aβ42-treated SH-SY5Y cells compared with Lit28i siRNA-transfected cells. Few dots of $pS^{194}$-FADD were sparingly and mainly distributed in the cytoplasm of PKR siRNA-transfected SH-SY5Y cells and exposed to Aβ42 (Fig. 6*C*).

The death receptor signaling pathway was related to the cleavage of pro-caspase-8 given the active form of caspase-8 able to cleave the procaspase-3 is caspase-3. In Fig. 7, activities of caspase-8 (*A*) and -3 (*B*) increased about 50–60% in Aβ-treated cells compared with untreated cells transfected with Interferin™ reagent alone or with Lit28i siRNA. However, PKR gene silencing significantly prevented the increase in both caspase-3 and -8 activities.

*Effect of the C16 Compound in Aβ-treated SH-SY5Y Cells*—The C16 compound is a specific inhibitor of the active form of PKR (19). Our previous studies reported under the same experimental conditions that 2 μM (10-fold of $IC_{50}$) C16 clearly inhibited the $pT^{451}$-PKR levels in Aβ42-treated SH-SY5Y cells (9). $pT^{451}$-PKR and $pS^{194}$-FADD were analyzed in nuclear extracts of SH-SY5Y cells pretreated with 2 μM C16 1 h before 20-μM Aβ42 treatment for 4 h by immunoblot. Under these experimental conditions, $pT^{451}$-PKR expression was decreased by 63% compared with cells preincubated with the vehicle and treated with Aβ42 (Fig. 8*A*). In the same time, $pS^{194}$-FADD expression was reduced by 65% (Fig. 8*B*). Total forms of PKR and FADD in cytoplasmic extracts of SH-SY5Y cells pretreated with C16 and treated with Aβ42 were comparable to those of corresponding cells not treated with Aβ42 (Fig. 8*D*).

A confocal staining confirmed that the C16 pretreatment prevented the staining of $pT^{451}$-PKR and $pS^{194}$-FADD induced by Aβ42 (Fig. 8*C*) compared with cells pretreated with the vehicle where $pT^{451}$-PKR and $pS^{194}$-FADD were intensively translocated in nuclei. Signals of $pT^{451}$-PKR and $pS^{194}$-FADD were weak and mainly cytoplasmic in control cells pretreated with vehicle and an extinction of the $pT^{451}$-PKR signal was observed in control cells pretreated with C16. Furthermore, this specific treatment completely prevented the activities of caspase-3 and -8 induced by Aβ42 treatment, whereas the negative C16 treatment showed an increase of about 50–55% as it was observed in vehicle control (Fig. 9, *A* and *B*).

## DISCUSSION

The PKR signaling pathway is largely described in AD (1, 2, 5–9). PKR is a serine-threonine kinase that phosphorylates the eIF2α factor, in response to various stress signals such as virus infection, pro-inflammatory stimuli, growth factors, and oxidative stress. Besides the down-regulation of translation, PKR can also induce apoptosis by affecting several signaling pathways (28). Indeed, many studies performed in virus-infected cells reported that PKR regulates p53 (29), nuclear factor-κB (NF-κB) (30), mitogen-activated protein kinases (MAPK) (31), FADD/caspase-8 (12, 32), signal transducers and activators of transcription (STAT) (33), and activating transcription factor 3 (ATF-3) (34). Interestingly, amyloid peptide excessively produced in AD, also induced activation of apoptotic signal transducers such as FADD/caspase-8 (35). Furthermore, many post-mortem studies showed the FADD-linked death receptor signaling pathway in the physiopathology of AD (15–17). However, the mechanism of control of the FADD/caspase-8 pathway by PKR is unknown in AD.

Here, we showed an intense nuclear translocation of $pT^{451}$-PKR in Aβ42-treated SH-SY5Y cells as described in $APP_{SL}PS1$ KI mouse brains and in AD patients (6, 9), which was associated with a clear nuclear translocation of $pS^{194}$-FADD. PKR contains nuclear localization signals (NLS), (36, 37). However, the role of PKR in the nucleus is not clearly understood. FADD is a well-known adaptor of two death receptors, Fas and tumor

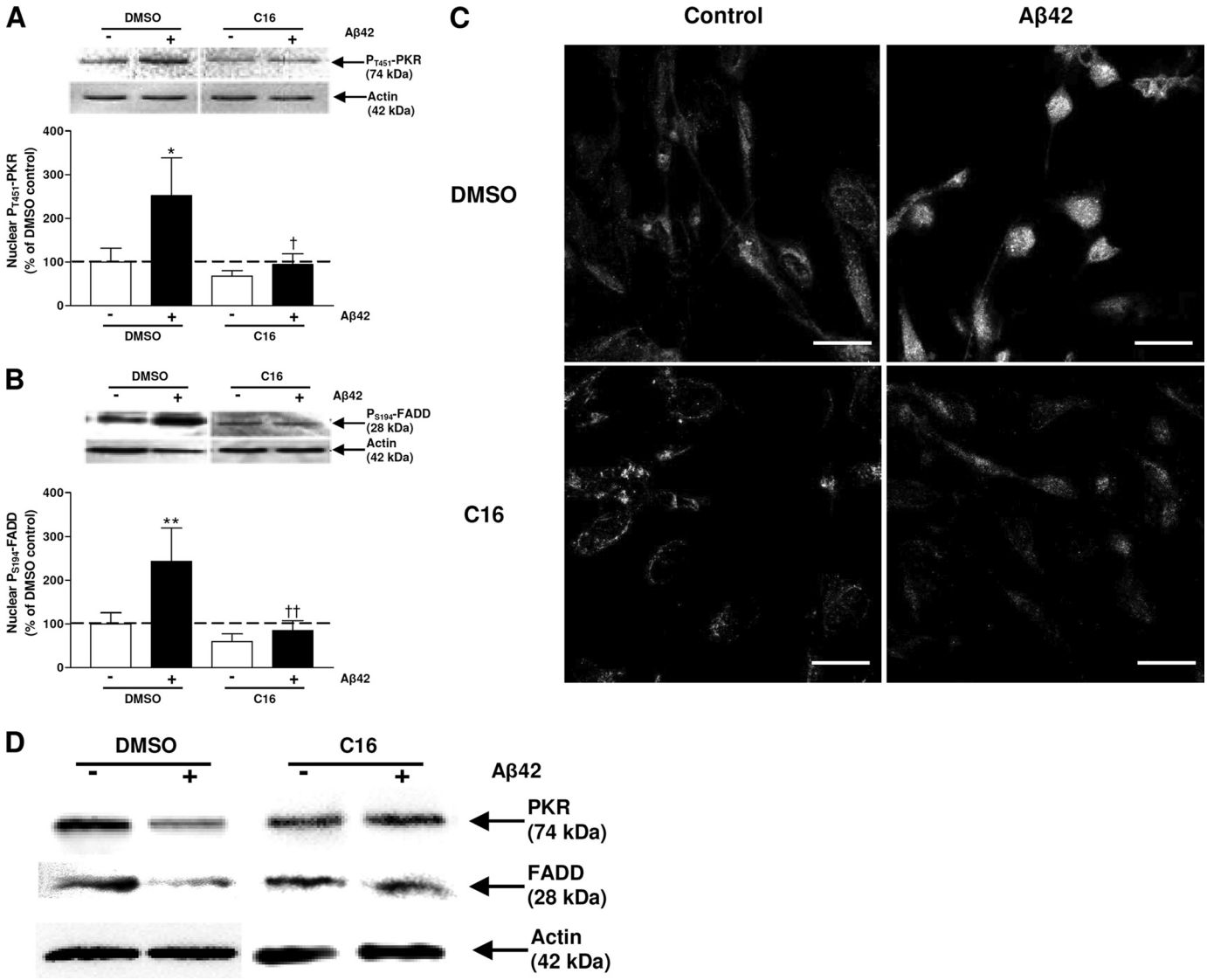


FIGURE 8. **Effects of a specific inhibitor of PKR in Aβ42-treated cells.** Representative blots show the immunoreactivity of $pT^{451}$-PKR (*A*), $pS^{194}$-FADD (*B*), and actin in nuclear extracts from SH-SY5Y cells pretreated with 2 μM C16 and exposed to Aβ42 for 4 h. The results are expressed as arbitrary units and are normalized compared with the DMSO control. Results are the mean ± S.E. of five independent experiments in duplicate. *, $p < 0.05$; **, $p < 0.01$ compared with control; and †, $p < 0.05$; ††, $p < 0.01$ compared with cells incubated with DMSO + Aβ42 by one-way ANOVA followed by Newman-Keuls' test for multiple comparisons. In *panel C*, a representative confocal staining in Aβ42-treated SH-SY5Y show that 2 μM C16 prevented nuclear $pT^{451}$-PKR and $pS^{194}$-FADD signals. *Bars*: 20 μm. In *panel D*, representative blots of total PKR and total FADD and corresponding actin in cytoplasmic extracts from SH-SY5Y cells pretreated with 2 μM of C16 and exposed to Aβ42 for 4 h are shown.

necrosis factor receptor-1 (TNFR-1), able to recruit and activate caspase-8 through its death-effector domain (DED). Furthermore, the authors showed NLS and nuclear export signals (NES) in the DED of the protein, suggesting the shuttle of FADD between nucleus and cytoplasm (38). Our results showed that PKR and FADD physically interacted in the nuclei of SH-SY5Y cells exposed to Aβ42, which was in three conformational states (monomers, oligomers, and fibrils) under our experimental conditions (see supplemental Fig. S1). It is difficult to say which Aβ42 state is more responsible for this PKR-FADD interaction, but after 4 h of exposure to Aβ42 there were more oligomers and a higher density of Aβ42 fibrils than after a 30-min incubation. Parallel to this interaction, there was a significant time-dependent increase in FasL levels in Aβ42-treated SH-SY5Y cells. FasL exhibits strong cytotoxic activity against Fas-expressing cells and is a potent activator of Fas-mediated cell death (39). The up-regulation of FasL induced by Aβ42 was in accordance with other Aβ neurotoxicity models (15). Further, the authors showed that FasL expression was remarkably elevated in senile plaques and neurofilament-positive dystrophic neurites and in association with active caspase-8 in the AD brain (15, 17). Our *in vitro* results were confirmed in the cortex of $APP_{SL}PS1$ KI transgenic mice where FasL expression and FADD activation were 4-fold and 2-fold higher than those in wild-type mice, respectively. The strong FasL labeling was in clustered spherical structures and in a distribution consistent with amyloid deposits as it was shown in AD brains (15). This increase of FasL was observed at 3 months of age before the massive neuronal loss described in $APP_{SL}PS1$ KI mice. Thus, both the early FasL production and its localization

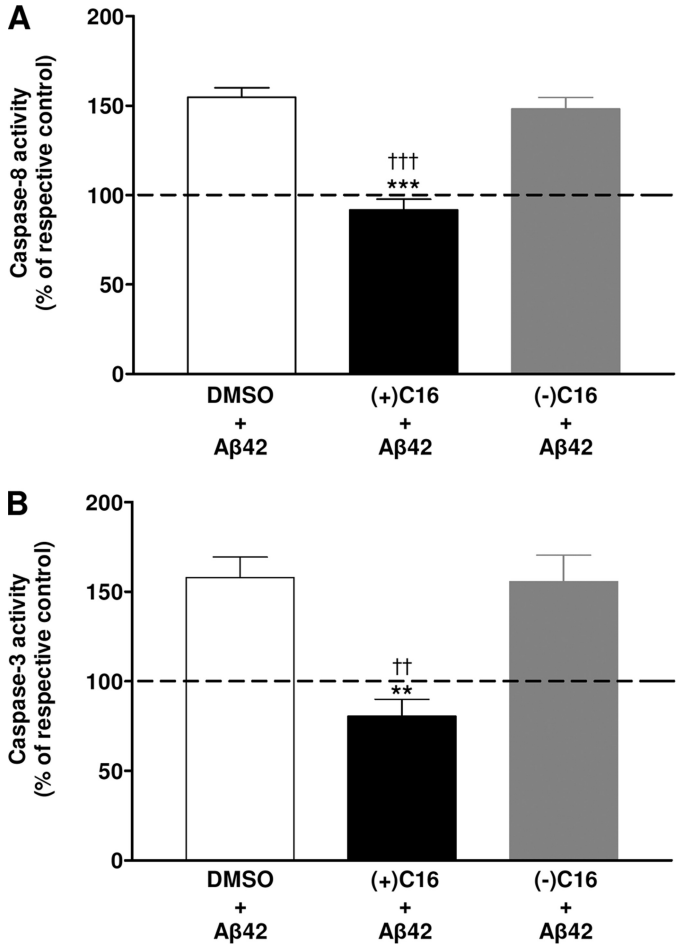


FIGURE 9. **Prevention of caspase-8 and -3 activities by C16 in A$\beta$42-treated SH-SY5Y cells.** Histograms show activities of caspase- 8 (*A*) and -3 (*B*) after pretreatment of SH-SY5Y cells either with vehicle (2% DMSO) or 2 $\mu$M positive PKR inhibitor [(+)C16] or 2 $\mu$M negative PKR inhibitor [(−)C16] and treatment of cells with A$\beta$42 for 4 h. *n*, each condition and each experiment, the activity of caspase-8 and -3 obtained in the presence of A$\beta$ was compared with that obtained without A$\beta$. Results represent the mean ± S.E. of five independent experiments in triplicate. Statistical analysis using a one-way ANOVA followed by the Newman-Keuls test revealed significative results; **, $p < 0.01$; ***, $p < 0.001$; and ††, $p < 0.01$; †††, $p < 0.001$ compared with vehicle and (−)C16 SH-SY5Y cells, respectively.

around diffuse amyloid deposits support the hypothesis that neuronal degeneration may be initiated in dystrophic neurons, possibly contributing to the loss of synapse-associated proteins in AD and/or retrogradely inducing the soma to degenerate.

Previously, we also showed the activation of PKR in the cortex of $APP_{SL}$PS1 KI associated with apoptotic neurons (9). As in A$\beta$42-treated SH-SY5Y cells, PKR and FADD physically interacted in cortex of $APP_{SL}$PS1 KI, strengthening the involvement of PKR/FADD signaling in the initiation of the neuronal death in AD. Indeed, this interaction was depicted at 3 months of age, where no neuronal loss was observed in these transgenic mice. However, $APP_{SL}$PS1 KI mice displayed a strong intraneuronal A$\beta$ immunostaining with diffuse amyloid deposits (21, 27, 40), suggesting the role of the intraneuronal A$\beta$ in the stimulation of the PKR/FADD signaling pathway.

By interacting with FADD, PKR could phosphorylate it to induce apoptosis. Both PKR gene silencing and a specific pharmacological inhibitory treatment significantly reduced not only the nuclear translocation of phosphorylated forms of PKR and FADD but also rescued SH-SY5Y cells from the active forms of caspase-3 and -8 induced by the A$\beta$42 treatment. Other reports demonstrated that primary cultured neurons from PKR knockout mice were less sensitive to A$\beta$42 neurotoxicity than those from wild-type mice (2) and that SH-SY5Y cells overexpressed a dominant-negative FADD construct (13) or neuronal cultures from mice carrying mutations in Fas or in FasL (15) exhibited protection from A$\beta$42 neurotoxicity. This study demonstrates for the first time the role of PKR in the death receptor signaling in AD as it was described in the host defense against virus infection (12, 32). The inhibition of PKR can trigger two neuroprotective benefits: first, the blockade of the extrinsic apoptotic pathway involving the FADD/caspase-8 pathway and second, its own activation by the inhibition of caspase-3, which was also activated by the mitochondrial dysfunction in AD (41). The caspase-3 inhibition could prevent the cleavage of PKR by caspase-3 and thus reduce active PKR N-terminal and C-terminal fragments playing a role in the activation of intact PKR (2, 5, 42). Both treatments investigated in our study are consistent with this last hypothesis, because the PKR siRNA transfection reduced by only one-third total PKR expression leading to a 60% inhibition of the nuclear A$\beta$42-induced $pT^{451}$-PKR levels and to a total inhibition of caspase-3 activity. The C16 treatment blocking the kinase domain of PKR also decreased to the same order the levels of $pT^{451}$-PKR and completely prevented caspase-3 activity. The maintenance of the PKR activation by the PKR fragments generated by caspase-3 would be highly attenuated. Besides, PKR can be activated by PKR-associated activator (PACT) in human or RAX in mouse (43, 44). However, no data were reported about the link between these PKR activators and membrane signal transduction. It is of interest to better understand factors involved between A$\beta$ production and the PKR activation. In addition to the prevention of cytoplasmic apoptotic factors, the PKR inhibition could knockdown not only nuclear PKR-induced apoptotic signal transducers (p53, NF-$\kappa$B, MAPK) but also the apoptotic role of FADD in the nucleus. Indeed, the nuclear localization of $pS^{194}$-FADD could be a way to induce apoptosis through its interaction with MBD4 (14) or with DED containing DNA-binding protein shutting off some nucleolar functions as the RNA polymerase I and II transcription (45, 46). Nevertheless, further studies are needed to determine the mechanistic basis of the presence of FADD in the nucleus in the physiopathology of AD.

In conclusion, these experiments demonstrate that PKR can control not only the FADD/caspase-8 signaling pathway but also the nuclear apoptotic role of phosphorylated FADD in A$\beta$ neurotoxicity. Furthermore, this study underlines the neuroprotective effects of PKR inhibitory treatment in the A$\beta$-induced apoptosis. Other studies showed that the down-regulation of PKR also prevented other apoptotic targets such as p53 (29), NF-$\kappa$B (30), MAPK (31), STAT (33), and ATF-3 (34). Some of these targets were also induced by the amyloid peptide that is excessively produced in AD (35, 47–51). Thus, it is necessary to start chronic treatment blocking active PKR in AD transgenic mice, because PKR controls many apoptotic signal transduction pathways described in AD, a serious problem in public health.

*Acknowledgments—We thank Anne Cantereau (CNRS-UMR6187, Poitiers, France), Nathalie Quellard, and Béatrice Fernandez (Department of Anatomy and Pathologic Cytology, Poitiers University Hospital) for expert assistance with confocal analysis and with scanning electron microscopy, respectively.*

## REFERENCES


1. Peel, A. L., and Bredesen, D. E. (2003) *Neurobiol. Dis.* **14,** 52–62
2. Chang, R. C., Suen, K. C., Ma, C. H., Elyaman, W., Ng, H. K., and Hugon, J. (2002) *J. Neurochem* **83,** 1215–1225
3. Lafay-Chebassier, C., Paccalin, M., Page, G., Barc-Pain, S., Perault-Pochat, M. C., Gil, R., Pradier, L., and Hugon, J. (2005) *J. Neurochem.* **94,** 215–225
4. Pei, J. J., and Hugon, J. (2008) *J. Cell Mol. Med.* **12,** 2525–2532
5. Suen, K. C., Yu, M. S., So, K. F., Chang, R. C., and Hugon, J. (2003) *J. Biol. Chem.* **278,** 49819–49827
6. Onuki, R., Bando, Y., Suyama, E., Katayama, T., Kawasaki, H., Baba, T., Tohyama, M., and Taira, K. (2004) *EMBO J.* **23,** 959–968
7. Chang, R. C., Wong, A. K., Ng, H. K., and Hugon, J. (2002) *Neuroreport* **13,** 2429–2432
8. Peel, A. L. (2004) *J Neuropathol Exp. Neurol.* **63,** 97–105
9. Page, G., Rioux Bilan, A., Ingrand, S., Lafay-Chebassier, C., Pain, S., Perault Pochat, M. C., Bouras, C., Bayer, T., and Hugon, J. (2006) *Neuroscience* **139,** 1343–1354
10. Paccalin, M., Pain-Barc, S., Pluchon, C., Paul, C., Besson, M. N., Carret-Rebillat, A. S., Rioux-Bilan, A., Gil, R., and Hugon, J. (2006) *Dement Geriatr Cogn Disord* **22,** 320–326
11. Damjanac, M., Page, G., Ragot, S., Laborie, G., Gil, R., Hugon, J., and Paccalin, M. (2009) *J. Cell Mol. Med.,* in press
12. Gil, J., and Esteban, M. (2000) *Oncogene* **19,** 3665–3674
13. Cantarella, G., Uberti, D., Carsana, T., Lombardo, G., Bernardini, R., and Memo, M. (2003) *Cell Death Differ.* **10,** 134–141
14. Screaton, R. A., Kiessling, S., Sansom, O. J., Millar, C. B., Maddison, K., Bird, A., Clarke, A. R., and Frisch, S. M. (2003) *Proc. Natl. Acad. Sci. U.S.A.* **100,** 5211–5216
15. Su, J. H., Anderson, A. J., Cribbs, D. H., Tu, C., Tong, L., Kesslack, P., and Cotman, C. W. (2003) *Neurobiol. Dis.* **12,** 182–193
16. Wu, C. K., Thal, L., Pizzo, D., Hansen, L., Masliah, E., and Geula, C. (2005) *Exp. Neurol* **195,** 484–496
17. Nishimura, T., Akiyama, H., Yonehara, S., Kondo, H., Ikeda, K., Kato, M., Iseki, E., and Kosaka, K. (1995) *Brain Res.* **695,** 137–145
18. Simmons, L. K., May, P. C., Tomaselli, K. J., Rydel, R. E., Fuson, K. S., Brigham, E. F., Wright, S., Lieberburg, I., Becker, G. W., Brems, D. N., *et al.* (1994) *Mol. Pharmacol.* **45,** 373–379
19. Jammi, N. V., Whitby, L. R., and Beal, P. A. (2003) *Biochem. Biophys. Res. Commun.* **308,** 50–57
20. Dignam, J. D., Lebovitz, R. M., and Roeder, R. G. (1983) *Nucleic Acids Res.* **11,** 1475–1489
21. Casas, C., Sergeant, N., Itier, J. M., Blanchard, V., Wirths, O., van der Kolk, N., Vingtdeux, V., van de Steeg, E., Ret, G., Canton, T., Drobecq, H., Clark, A., Bonici, B., Delacourte, A., Benavides, J., Schmitz, C., Tremp, G., Bayer, T. A., Benoit, P., and Pradier, L. (2004) *Am. J. Pathol.* **165,** 1289–1300
22. Damjanac, M., Rioux Bilan, A., Paccalin, M., Pontcharraud, R., Fauconneau, B., Hugon, J., and Page, G. (2008) *Neurobiol Dis.* **29,** 354–367
23. Romano, P. R., Garcia-Barrio, M. T., Zhang, X., Wang, Q., Taylor, D. R., Zhang, F., Herring, C., Mathews, M. B., Qin, J., and Hinnebusch, A. G. (1998) *Mol. Cell. Biol.* **18,** 2282–2297
24. Scaffidi, C., Volkland, J., Blomberg, I., Hoffmann, I., Krammer, P. H., and Peter, M. E. (2000) *J. Immunol.* **164,** 1236–1242
25. Chen, G., Bhojani, M. S., Heaford, A. C., Chang, D. C., Laxman, B., Thomas, D. G., Griffin, L. B., Yu, J., Coppola, J. M., Giordano, T. J., Lin, L., Adams, D., Orringer, M. B., Ross, B. D., Beer, D. G., and Rehemtulla, A. (2005) *Proc. Natl. Acad. Sci. U.S.A.* **102,** 12507–12512
26. Christensen, K. D., Roberts, J. S., Royal, C. D., Fasaye, G. A., Obisesan, T., Cupples, L. A., Whitehouse, P. J., Butson, M. B., Linnenbringer, E., Relkin, N. R., Farrer, L., Cook-Deegan, R., and Green, R. C. (2008) *Genet. Med.* **10,** 207–214
27. Barrier, L., Ingrand, S., Fauconneau, B., and Page, G. (2008) *Neurobiol Aging,* in press
28. Garcíia, M. A., Gil, J., Ventoso, I., Guerra, S., Domingo, E., Rivas, C., and Esteban, M. (2006) *Microbiol. Mol. Biol. Rev.* **70,** 1032–1060
29. Cuddihy, A. R., Wong, A. H., Tam, N. W., Li, S., and Koromilas, A. E. (1999) *Oncogene* **18,** 2690–2702
30. Gil, J., Alcamí, J., and Esteban, M. (2000) *Oncogene* **19,** 1369–1378
31. Goh, K. C., deVeer, M. J., and Williams, B. R. (2000) *EMBO J.* **19,** 4292–4297
32. Balachandran, S., Kim, C. N., Yeh, W. C., Mak, T. W., Bhalla, K., and Barber, G. N. (1998) *EMBO J.* **17,** 6888–6902
33. Ramana, C. V., Grammatikakis, N., Chernov, M., Nguyen, H., Goh, K. C., Williams, B. R., and Stark, G. R. (2000) *EMBO J.* **19,** 263–272
34. Guerra, S., López-Fernández, L. A., García, M. A., Zaballos, A., and Esteban, M. (2006) *J. Biol. Chem.* **281,** 18734–18745
35. Ivins, K. J., Thornton, P. L., Rohn, T. T., and Cotman, C. W. (1999) *Neurobiol. Dis.* **6,** 440–449
36. Garcia-Bustos, J., Heitman, J., and Hall, M. N. (1991) *Biochim. Biophys. Acta* **1071,** 83–101
37. Jeffrey, I. W., Kadereit, S., Meurs, E. F., Metzger, T., Bachmann, M., Schwemmle, M., Hovanessian, A. G., and Clemens, M. J. (1995) *Exp. Cell Res.* **218,** 17–27
38. Gómez-Angelats, M., and Cidlowski, J. A. (2003) *Cell Death Differ* **10,** 791–797
39. Nagata, S., and Golstein, P. (1995) *Science* **267,** 1449–1456
40. Bayer, T. A., Breyhan, H., Duan, K., Rettig, J., and Wirths, O. (2008) *Neurodegener. Dis.* **5,** 140–142
41. Engidawork, E., Gulesserian, T., Yoo, B. C., Cairns, N., and Lubec, G. (2001) *Biochem. Biophys. Res. Commun.* **281,** 84–93
42. Kalai, M., Suin, V., Festjens, N., Meeus, A., Bernis, A., Wang, X. M., Saelens, X., and Vandenabeele, P. (2007) *Cell Death Differ.* **14,** 1050–1059
43. Bennett, R. L., Blalock, W. L., and May, W. S. (2004) *J. Biol. Chem.* **279,** 42687–42693
44. Patel, R. C., and Sen, G. C. (1998) *EMBO J.* **17,** 4379–4390
45. Stegh, A. H., Schickling, O., Ehret, A., Scaffidi, C., Peterhänsel, C., Hofmann, T. G., Grummt, I., Krammer, P. H., and Peter, M. E. (1998) *EMBO J.* **17,** 5974–5986
46. Zheng, L., Schickling, O., Peter, M. E., and Lenardo, M. J. (2001) *J. Biol. Chem.* **276,** 31945–31952
47. Checler, F., Sunyach, C., Pardossi-Piquard, R., Sévalle, J., Vincent, B., Kawarai, T., Girardot, N., St George-Hyslop, P., and da Costa, C. A. (2007) *Curr. Alzheimer Res.* **4,** 423–426
48. Buggia-Prevot, V., Sevalle, J., Rossner, S., and Checler, F. (2008) *J. Biol. Chem.* **283,** 10037–10047
49. Uberti, D., Lanni, C., Racchi, M., Govoni, S., and Memo, M. (2008) *Neurodegener. Dis.* **5,** 209–211
50. Chiba, T., Yamada, M., Sasabe, J., Terashita, K., Shimoda, M., Matsuoka, M., and Aiso, S. (2009) *Mol. Psychiatry* **14,** 206–222
51. Zhu, X., Lee, H. G., Raina, A. K., Perry, G., and Smith, M. A. (2002) *Neurosignals* **11,** 270–281